

Study of EphA2 dimerization and clusterization in living cells using sensitized acceptor emission in FRET pair

G.V. Sharonov^{1,2}, M.N. Mozgovaja², M.V. Astapova¹, P.M. Kolosov¹, A.S. Arseniev¹ and A.V. Feofanov^{1,3}

¹Shemyakin-Ovchinnikov Institute of Bioorganic Chemistry, Russian Academy of Sciences, ul. Miklukho-Maklaya 16/10, 117997, Moscow, Russia

²Faculty of Fundamental Medicine, Lomonosov Moscow State University, Lomonosov ave., 31/5, 119192, Moscow, Russia

³Biological Faculty, Lomonosov Moscow State University, Vorobyevi Gori 1, 119991, Moscow, Russia

Ligand induced activation of ephrin receptor EphA2 proceeds through receptor dimerization and phosphorylation followed by activation of effector kinases and triggering intracellular signaling pathways. Human embryonic kidney 293T (HEK293T) cells have been obtained by us that stably expressed CFP- and YFP- tagged EphA2. We report on the studies of EphA2 in HEK293T cells with confocal laser scanning microscopy and flow cytometry. We demonstrate that sensitized acceptor emission (SAE) technique reveals dimerization of CFP-EphA2 and YFP-EphA2 due to Förster resonance energy transfer (FRET) between CFP and YFP. The SAE technique was successfully used by us to follow dimerization and clusterization of EphA2 in single living cells in real time. To improve FRET analysis we have developed an ImageJ plugin for data processing and performed SAE measurements on basal cell membrane, where largest part of plasma membrane is simultaneously in focus. We report on pulse-like character of EphA2 dimerization on plasma membrane after stimulation of cells with ephrinA3. The maximal level of EphA2 dimerization was detected in 5 min after the stimulation and decreased to the basal level in 20-25 min. Similar kinetic profile was observed in the EphA2 phosphorylation measurements with flow cytometry on fixed HEK293T cells. Our data confirm tentatively the concept that homophilic interactions (i.e. dimerization), clusterization and phosphorylation are closely interrelated steps of the ligand-induced activation of EphA2.

Keywords receptor tyrosine kinases; FRET; EphA2; ephrin

1. Introduction

1.1 Overview of receptor tyrosine kinases activation assays

Receptor tyrosine kinases (RTK) comprise a large class of receptors including growth factor receptors, insulin receptor, and cell guidance Eph receptors [1]. Ligand binding induces formation of RTK dimers and higher order homophilic complexes that allow the kinase domain to trans-phosphorylate neighbor receptors in the complex. Phosphorylated RTK attract to the site of activation and activate effector kinases that in their turn trigger complex intracellular molecular signaling pathways and finally affect cell proliferation, adhesion, migration, and gene expression.

Development of RTK-targeted drugs needs an assay that measures RTK activation. Correct stoichiometry, orientation and membrane association of RTK active complexes can be achieved with cell-based assays only. Currently, conventional cell-based methods for the RTK activation measurement utilize phosphorylation of the receptor itself or its effector kinases as readout. However, phosphorylation assays have some disadvantages. They are time and reagent consuming, disregard individual cell peculiarities and ignore existence of multiple phosphorylation sites with different, often unknown functions. Sometimes phosphorylation of target RTK can be an indirect effect resulting from the activation of other signaling pathways.

Another promising assay is realized with the enzyme complementation technology. RTK and its effector kinase are fused with two parts of an enzyme that show little or no spontaneous association (PathHunter assay from DiscoverX [2]). Alternatively, both parts of enzyme can be fused with RTK [3]. RTK activation forces enzyme complementation, and the arising enzyme activity is detected using a chemiluminescent substrate.

Enzymes used in the enzyme complementation technology have large molecular weight (for example, β -galactosidase is 464 kDa enzyme) and may alter activity of fused proteins. To diminish this effect on RTK, RTK is fused with smaller part of split enzyme. But the effector kinase fused with larger part of split enzyme still have artificially high molecular weight that can very likely disturb normal signal transduction and feedback loops crucial for RTK activity regulation.

Current advances in fluorescent techniques provide multiple powerful approaches to various fields of science and technology [4]. Time-resolved fluorescence, fluorescence polarization, Förster resonance energy transfer (FRET) are widely used in cell-free high throughput assays for RTK activation [5]. Rapid progress in cell-based fluorescence techniques was initiated by the development of genetically encoded fluorescence proteins (FP) in mid-90s. Great advantage is that FP can be fused with a target protein or functionalized with a peptide and expressed endogenously in cells. Today's arsenal of FP-based assays includes photoactivated and photoconvertible proteins, cell-timers, protein maturation and degradation probes as well as different sensors for specific enzymatic activity, membrane potential and

intracellular chemical analytes [6]. FP progress is complemented with development of fluorescence microscopy techniques that allow detection of multiple FP with submicron resolution in individual living cells.

FRET is the gold-standard fluorescence technique to detect molecular interaction. It is very attractive for discerning RTK dimerization and/or RTK interactions with effector kinases in cell-based systems. FRET application in cell-based assays is especially promising for real time probing of protein interactions but coupled with some complexity as discussed below.

An alternative fluorescence approach to discerning protein-protein interactions in living cells is bimolecular fluorescence complementation (BiFC) assay [6]. FP is split into two non-fluorescent parts that are fused with two target proteins. Interaction of target proteins induces FP reconstitution and fluorescence appearance. The BiFC assay allows detection of very weak interactions but is unsuitable for real-time detection of target protein interactions, because maturation of fluorescent chromophore in reconstituted FP takes time (minutes to hours) [6]. Note, that the FP reconstitution is irreversible in most cases.

1.2 FRET-based assays of RTK activation

FRET provides a reliable and powerful technique for detection of protein-protein interactions. FRET represents physical phenomenon when energy absorbed by one molecule (donor) instead of being emitted as fluorescence is transferred to the neighboring molecule (acceptor). FRET occurs only when emission spectrum of donor overlaps the absorption spectrum of acceptor (FRET pair) and distance between these two molecules is shorter than *ca.* 10 nm.

Accurate measurement of FRET requires that a contribution of so called spontaneous FRET is taken into account. Spontaneous FRET arises when donor and acceptor meet during diffusion and occurs without formation of complexes between donor- and acceptor- bearing molecules. It is realized because the excited state lifetime of fluorochromes is much shorter than the diffusion rate for most molecules. Probability of spontaneous FRET increases as a function of fluorochrome concentration. In solution spontaneous FRET is observed at millimolar concentrations of donor and acceptor. In membrane it is high when one acceptor is per 100-200 phospholipids, and donor is in excess [4]. Usually physiological protein concentrations and concentrations used in biological assays are much less than those required for spontaneous FRET, and FRET appearance is the strong indication of specific donor-acceptor interactions.

Both in cells and cell-free systems FRET measurements are facilitated with FRET-based sensors, special molecular constructions where donor and acceptor are coupled together at the strict 1/1 molar ratio. Specific molecular interactions induce characteristic changes in the spectral properties of a FRET-sensor. In fact most of the protein-based phosphorylation sensors use FRET reporter mechanism [7]. As a rule these sensors unite a tyrosine residue and a phosphorylated tyrosine (pTyr) recognizing domain (such as SH2 or PH), i.e. sense phosphorylation of themselves. To our knowledge there are no sensors to measure specific RTK phosphorylation in cells.

As was mentioned above activation of particular RTK can be detected in cells with specific antibodies recognizing one of pTyr on target RTK. To reveal all phosphorylated tyrosines of RTK, FRET technique and fluorescently labeled antibodies such as PY20 or PY72 can be used [8]. Here FP fused with target RTK serves as the second fluorochrome in FRET pair. However this method needs cell fixation, permeabilization and additional staining and thereby does not allow real-time measurements.

To utilize FRET for measurement of RTK dimerization during activation one part of the receptor needs to be fused with a donor and another with an acceptor [9]. In this case no additional sample manipulations or usage of sophisticated sensing agents are required. In spite of apparent simplicity of such approach there are only few works where it is used for detecting dimerization of RTK or other receptors. Successful examples include detection of dimerization of RTK α [9], chemokine GPCR receptor CXCR4 [10] and EGFR (by homo-FRET i.e. donor is identical to acceptor) [11].

1.3 Microscopy techniques for FRET measurements

In spite of robustness of FRET as indicator of molecular interactions its correct measurement remains a challenging task. Several approaches exist to detect FRET with subcellular resolution. One of the most reliable is fluorescence lifetime imaging microscopy (FLIM) [8, 12]. It utilizes the fact that donor fluorescence lifetime decreases when FRET occurs. FLIM primary advantage is independence of protein concentration. The limiting factor of FLIM application is sophisticated methodology and expensive equipment, which is not widely available yet to cell biology laboratories [12,13].

Another technique that detects FRET independently of concentration is fluorescence anisotropy imaging microscopy (FAIM) [11,14]. FAIM utilizes polarized light that excites donors with specific orientations of dipole moments. In the case of proteins, their large size restricts molecular rotation during excited state lifetime, and polarization of emitted fluorescence is similar to that of the excitation light (large anisotropy). When FRET is realized, fluorescence is emitted by acceptor and is depolarized (reduced anisotropy). The anisotropy value serves as indication of FRET. Since FRET recognition does not rely on spectral properties of fluorochromes, FAIM can be used for detection of both hetero-FRET (donor and acceptor are different fluorochromes) and homo-FRET (donor and acceptor are like fluorochromes) [11]. But in biological assays anisotropy change is relatively weak that makes detection of FRET with FAIM less reliable than with FLIM. FAIM can be combined with FLIM to gain advantages of both methods and improve robustness [11].

Most straightforward (but still not failsafe) FRET technique is the method of sensitized acceptor emission (SAE) at donor excitation realized with confocal laser scanning microscopy (CLSM). FRET measurements with SAE approach are rather simple when there are no direct excitation of acceptor with the wavelength used for donor excitation as well as no contribution of donor fluorescence in the acceptor detection channel (so called crosstalk or bleed-through) and *vice versa*. But at least among FPs we do not know such ideal donor-acceptor pairs. Usually all numerous SAE-based analytical routines take into account and introduce correction for the crosstalks and direct excitation of acceptor.

To apply SAE technique it is necessary to acquire three images including the distribution of acceptor emission at the acceptor excitation (subscript 3 in eq. 1-4) as well as the distributions of donor and acceptor emissions at donor excitation (subscripts 1 and 2, respectively). General crosstalk compensation contains mutual corrections of donor, acceptor and SAE signal (coefficients α_{nm} in eq. 1). SAE signal bleed-through can be set to zero ($\alpha_{12} = \alpha_{32} = 0$) in many cases. Moreover, most of FRET calculation programs discard crosstalk between donor and acceptor ($\alpha_{31} = \alpha_{13} = 0$) and account only for donor and acceptor crosstalks with SAE signal [15,16]. To calculate crosstalks of donor and acceptor (coefficients α_{21} , α_{31} , α_{13} and α_{23}) the samples with donor alone and acceptor alone are measured, and equations 2 and 3 are applied. A system of three linear equations with three unknowns should be solved for each scanned point of the sample in order to get SAE signal value (i.e. FRET value) in each point (eq. 4). Since these computations multiply any errors and noise introduced during acquisition, image measurements and their processing should be carried very accurately. Probable sources of errors are: nonlinearity and saturation of fluorescence detection, cellular autofluorescence, non-uniform background, excitation intensity fluctuations, sample drift and cell motility. Several approaches were proposed to eliminate some of these errors [15–18].

$$\text{General crosstalk compensation: } \begin{pmatrix} I_1 \\ I_2 \\ I_3 \end{pmatrix} = \begin{pmatrix} 1 & \alpha_{12} & \alpha_{13} \\ \alpha_{21} & 1 & \alpha_{23} \\ \alpha_{31} & \alpha_{32} & 1 \end{pmatrix} \begin{pmatrix} I_D \\ I_{FRET} \\ I_A \end{pmatrix} \quad (1),$$

$$\text{donor alone: } \begin{pmatrix} I_1 \\ I_2 \\ I_3 \end{pmatrix} = \begin{pmatrix} 1 & 0 & \alpha_{13} \\ \alpha_{21} & 1 & \alpha_{23} \\ \alpha_{31} & 0 & 1 \end{pmatrix} \begin{pmatrix} I_D \\ 0 \\ 0 \end{pmatrix} \quad (2),$$

$$\text{acceptor alone: } \begin{pmatrix} I_1 \\ I_2 \\ I_3 \end{pmatrix} = \begin{pmatrix} 1 & 0 & \alpha_{13} \\ \alpha_{21} & 1 & \alpha_{23} \\ \alpha_{31} & 0 & 1 \end{pmatrix} \begin{pmatrix} 0 \\ 0 \\ I_A \end{pmatrix}; \quad (3),$$

$$\text{donor + acceptor: } \begin{pmatrix} I_1 \\ I_2 \\ I_3 \end{pmatrix} = \begin{pmatrix} 1 & 0 & \alpha_{13} \\ \alpha_{21} & 1 & \alpha_{23} \\ \alpha_{31} & 0 & 1 \end{pmatrix} \begin{pmatrix} I_D \\ I_{FRET} \\ I_A \end{pmatrix}, \quad (4),$$

where I_1 , I_2 , I_3 are measured fluorescence intensity values in corresponding images, and I_D , I_A , I_{SAE} are real (corrected) signals of donor, acceptor and SAE, respectively.

Here, we report on the studies of ephrin receptor EphA2 in HEK293T cells stably transfected with CFP- and YFP-tagged EphA2. We show that SAE technique can be used to evaluate activation-induced dimerization of EphA2 in living cells, and to follow dimerization and clusterization of EphA2 in single living cells in real time. We report on pulse-like character of receptor dimerization after stimulation of cells with ephrinA3. The maximal level of EphA2 dimerization was detected in 5 min after stimulation and decreased to the basal level in 20 min. Similar receptor activation kinetics was confirmed by EphA2 phosphorylation measurements thus approving validity of our FRET-based approach to study functioning of EphA2 receptors in living cells.

2. Experimental

2.1 Plasmids

To get the gene of EphA2, total cellular RNA from human breast adenocarcinoma MCF-7 cell line (10^6 cells from culture) was prepared by the guanidine thiocyanate method [19]. RNA for cDNA synthesis was treated with DNaseI (Boehringer) for 30 min at 37°C followed by phenol: chloroform extraction and ethanol precipitation. cDNA was synthesized from primer oligo-dT₁₆, on 500 ng total RNA. The reaction was performed with 0.2 mM dNTPs, 50U MMLV reverse transcriptase (Life Technologies), and 25 pmol oligo-dT₁₆ primer. The mixture was incubated at RT for 10 min, and polymerisation of first strand cDNA was performed at 37 °C for 1 h. The material was then heated to 95°C for 5 min. The reverse transcriptase reaction was then used for different polymerase chain reactions (PCR) run.

Plasmids with fused EphA2-CFP and EphA2-YFP were obtained as follows. Primers with restriction sites for *Bgl*III and *Sall* were used for EphA2-YFP chimera: 5'- TTTAGATCTATGGAGCTTCAGGCAGCCCCGC-3' and 5'-TTTGTCGACATGGGGATCCCCACAGTGTTC-3'. For EphA2-CFP chimera we used primers with *Xho*I and *Xba*I restriction sites: 5'- TTACTCGAGATGAGCGGGGCGAGGA-3' and 5'-ATTCTAGATTAGCGGTACAGCTCGTCCATG-3'. PCR reaction buffer contained 2.0 mM MgCl₂, 0.2 mM dNTPs, 5% DMSO, 1 U Pfu-Turbo Polymerase (Stratagene), 20 pmol of each primers and 1 µl of reverse transcriptase was used as template in the final

volume of 50 μL . The amplification was performed on a Thermo cycler (Perkin Elmer) in 40 cycles; 95 °C for 30 s, 69 °C for 30 s, 72 °C for 3.5 min, followed by 72 °C for 5 min. Four microliters of the PCR products were analyzed on a 1% polyacrylamide gel. Band corresponding the length of ephA2 gene (2900 nt) was excised from the gel and eluted by PCR extraction kit (Promega) in 50 μL of water. PCR fragment was hydrolysed with corresponding restriction endonucleases and cloned in pTagYFP-N (Evrogen) or pcDNA3-CFP (Addgene), treated with the same enzymes. Cloned ephA2 gene from cDNA was sequenced with the Sequenase kit (Amersham Biosciences).

2.2 Cells and their analysis

HEK293T cells were cultured in DMEM culture medium with low glucose and sodium pyruvate (HyClone) supplemented with 10% fetal bovine serum (FBS, HyClone). One day before transfection cells were seeded in the 6-well plate. Cells were transfected with 1 μg of plasmid mixed with 2.5 μl of lipofectamine 2000 (Invitrogen) per well. One-two days after that the transfected cells were harvested using Versene solution (Paneco) and analysed or sorted for further culture.

For CLSM experiments cells were seeded in wells of the 8-well Lab-Tek chambered cover glass (Nunc) covered with rat tail collagen (BD Biosciences) one day prior analysis. Cells were transferred to FBS-free culture medium in 4-8 h before EphA2 stimulation. For EphA2 stimulation we used ephrinA3 heterodimer with human Fc fragment (ephrinA3-Fc, R&D Systems) at the 10 $\mu\text{g}/\text{ml}$ final concentration.

CFP- of YFP-positive cells were selected with fluorescence activated cell sorting on MoFlo cell sorter (DakoCytomation) using the 405 nm diode laser (95 mW, Newport) and the 488 nm line of Ar⁺ laser (Enterprise II, Coherent). Selection during 4-6 week (4 sorting procedures) was used to get a cell line with stable expression of EphA2-CFP and/or EphA2-YFP. Cells with stable expression of EphA2-CFP were cloned and several clones were obtained. One of these clones was used for most described experiments. Cell lines with stable expression of EphA2-YFP or both chimeras were obtained using “wild type” HEK293T cells or one of EphA2-CFP expressing clones, respectively.

For flow cytometry analysis of EphA2 phosphorylation cells were detached with Versene solution after 4-5 h deprivation and resuspended in PBS at a final concentration 2-4 \times 10⁶ cells/ml. Cells were activated with the 10 $\mu\text{g}/\text{ml}$ ephrinA3-Fc for indicated time. After stimulation cells were fixed with paraformaldehyde (Sigma-Aldrich), permeabilized (Perm/Wash solution, BD Biosciences) and stained with anti-phospho-EphA2 primary antibodies (Abcam) and DyLight-488- or DyLight-649- labeled secondary antibodies (Jackson Immunoresearch). FACSCanto II flow cytometer (BD Biosciences) was used for the analysis.

CLSM images were obtained with either LSM510META (CarlZeiss, Jena, Germany) or TCS SP2 (Leica, Wetzlar, Germany). Both microscopes were equipped with thermo- and CO₂- controlled incubators. Live cell imaging was performed in Hank's solution at 37 °C. EphrinA3-Fc (4-20 μl) was added to cells during time-lapse measurements, and the medium was gently pipetted. CFP and YFP were excited with 458-nm and 514-nm wavelength of Ar⁺ laser, respectively. In order to obtain precise superposition of CFP, YFP and FRET images and reduce crosstalk, the alternate excitation of CFP and YFP was used in the “line-by-line” mode. Fluorescence of other fluorochromes was excited and detected at appropriate excitation and emission wavelengths using the regime of consecutive measurements (one fluorochrome per scanning frame).

FRET intensity in our experimental setup turned out to be relatively dim. This did not allow us to use available FRET analysis software (ImageJ plugins, Leica FRET software). We have created a special ImageJ (rsbweb.nih.gov/ij/) plugin allowing correction of FRET signal for contribution of crosstalk between CFP and YFP. This plugin takes into account CFP bleed-through into YFP channel and *vice versa*, treats image stacks and time-series, excludes pixels, where one of the channels is saturated and allows treatment of images having greyscales up to 32-bit. The plugin with description and example can be found at cytometry.ru/interactive-fret.html.

3. Results

3.1 Flow cytometry study of EphA2 phosphorylation in HEK293T cells

To evaluate functional activity and activation kinetics of EphA2 in new cell lines expressing EphA2 fused with FP we analyzed EphA2-CFP (EphA2-YFP) phosphorylation as a function of time after receptor stimulation with ephrinA3-Fc. Phosphorylated form of EphA2 (pEphA2) was detected by flow cytometry using rabbit anti-(pTyr588 and pTyr596) antibodies and DyLight-488 or DyLight649-labeled anti-rabbit secondary antibodies (Fig. 1A). These experiments revealed that a part of EphA2-CFP and EphA2-YFP was phosphorylated in cells even without activation of the receptors with a ligand (Fig. 1B, compare “HEK293T Con” and “Before”). EphA2 phosphorylation reached a maximum in 2-5 min after stimulation of cells with ephrinA3-Fc, and the response amplitude was *ca.* 3-fold higher than the level of background phosphorylation. EphA2 phosphorylation declined almost to the background level (Fig. 1B) in *ca.* 20 minutes after stimulation. These data indicate that EphA2-CFP and EphA2-YFP are functionally active in cells, and ligand-induced phosphorylation of EphA2 has a pulse-like character.

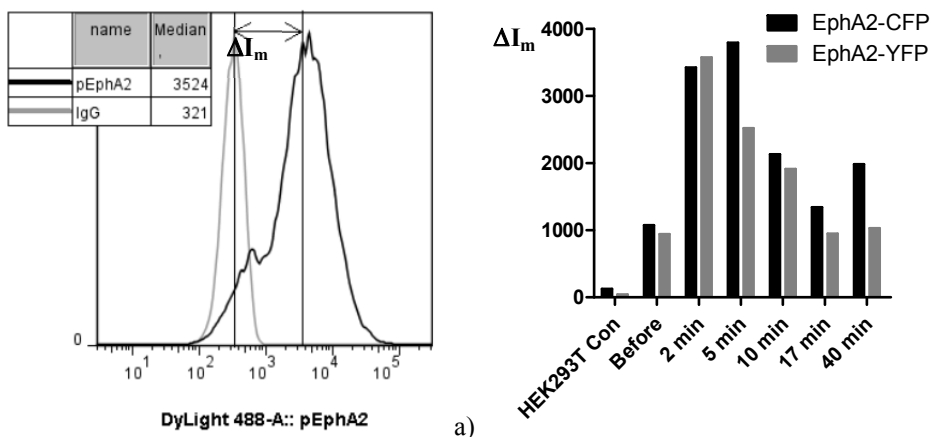


Fig.1 Flow cytometry data on phosphorylation of EphA2-CFP and EphA2-YFP after stimulation of cells with ephrinA3-Fc. a). Histograms of EphA2-CFP expressing cell distribution after staining with anti-pEphA2 antibodies (black curve) and isotypic IgG (grey curve) and anti-rabbit IgG-DyLight488. Vertical lines represent the median values, and an arrow shows the difference between medians of pEphA2 and IgG staining (ΔI_m). ΔI_m is used as a measure of EphA2 phosphorylation. b). EphA2 phosphorylation in wild cells (HEK293T Con), EphA2-CFP and EphA2-YFP expressing cells before addition of ephrinA3-Fc (Before) and in different time intervals after addition of 10 μ g/ml ephrinA3-Fc.

3.2 EphA2 localization in HEK293T cells

Localization of EphA2 in cells expressing EphA2 fused with FP was examined with CLSM. Analysis of different cell clones expressing EphA2-CFP revealed two types of EphA2-CFP cellular localization: homogeneous distribution over plasma membrane (PM) and granular cytoplasmic localization. Relative contribution of these two patterns in the overall receptor distribution depended on a cell clone. The same distribution patterns were found for EphA2-YFP, but PM localization prevailed.

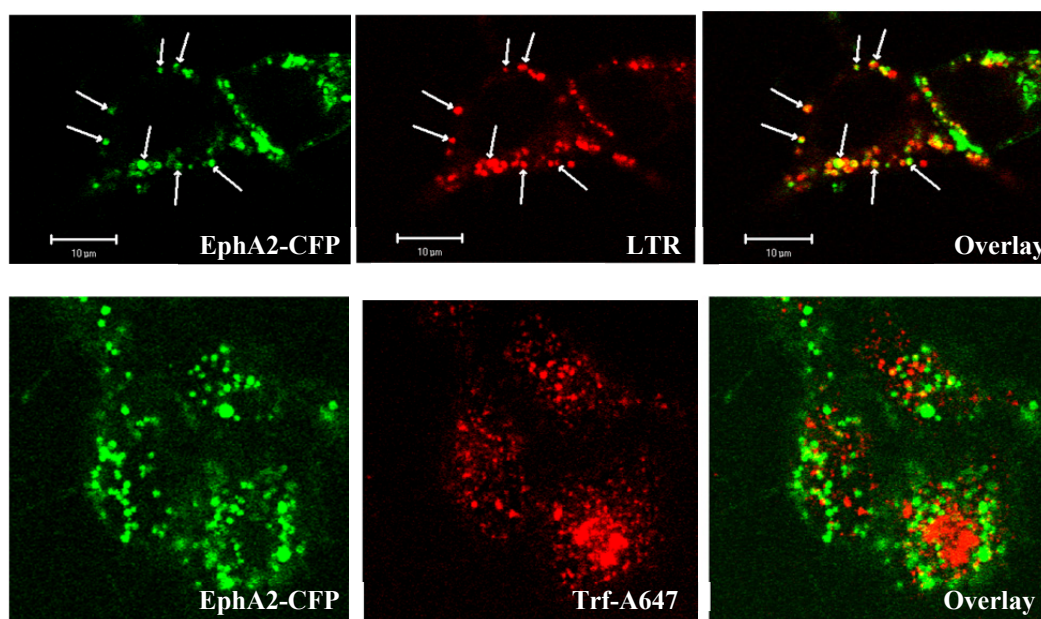


Fig. 2 Intracellular localization of EphA2 in HEK293T cells. Colocalization analysis of EphA2-CFP and selective fluorescent markers of lysosomes (LTR) and clathrin endosomes (Trf-A647). Distributions of EphA2-CFP (green) and an organelle marker (red) as well as overlay of these two distributions are presented in left, middle and right panels, respectively.

In order to reveal the origin of cytoplasmic vesicles containing EphA2 we used selective fluorescent markers for lysosomes (LysoTracker Red, LTR, Invitrogen) and clathrin endosomes (Transferrin-Alexa647, Trf-A647, Invitrogen). A cell clone with the dominant cytoplasmic localization of EphA2-CFP was used for these experiments. We found a partial colocalization of the EphA2-CFP containing vesicles with lysosomes and almost no their colocalization with clathrin endosomes (Fig. 2).

Mobility of EphA2 on PM was evaluated with the fluorescence recovery after photobleaching (FRAP) technique. Local tear in homogeneous PM staining produced after 2 min photobleaching was fully filled in with EphA2-YFP fluorescence within next 90 seconds (Fig. 3). This result indicates that EphA2 can freely diffuse over PM.

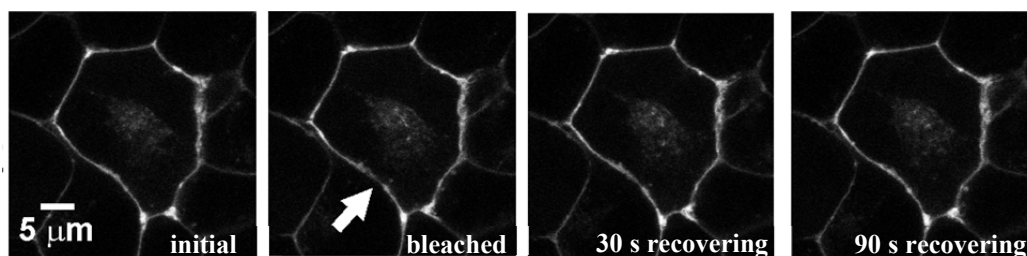


Fig. 3 Analysis of EphA2-YFP mobility in PM with FRAP technique. EphA2-YFP was bleached in a region indicated with an arrow (compare panels “initial” and “bleached”). Within next 90 s fluorescence in the bleached region is fully recovered due to fast membrane diffusion of EphA2-YFP.

3.3 Study of ligand induced activation of EphA2 in living HEK293T cells

To study ligand-induced dimerization of EphA2 cells stably expressing both EphA2-CFP and EphA2-YFP were obtained. The new cell line retains high EphA2-CFP expression and activity as well as has a broad range of donor/acceptor ratios due to variable expression of EphA2-YFP.

To measure FRET between EphA2-CFP and EphA2-YFP in living cells the SAE technique was used. Since intensity of SAE was relatively weak it was crucial to filter out every background. It was also important to perform measurements of CFP and YFP fluorescence almost simultaneously, i.e. within a second or less, and avoid in this way changes in receptor localization leading to wrong correction for CFP and YFP crosstalks. To control the accuracy of FRET detection we analyzed cells that expressed only EphA2-CFP or EphA2-YFP. The analysis was performed before and after stimulation of the cells with ephrinA3-Fc. As expected these cells gave a zero signal in the FRET images after correction for crosstalk (data not shown). Another evidence for reliability of SAE measurements is that FRET signal was highly sensitive to the level of EphA2-YFP expression. Thus, intensive FRET was observed in the cells with highest EphA2-YFP expression (Fig. 4 b).

Formation of ligand-EphA2 complexes was analyzed by us within the basal layer of PM (i.e. PM attached to the glass surface). The basal layer is the largest flat PM plane that can be imaged within a single optical slice using CLSM. Note, contacts between PM and a glass are realized with multiple membrane protuberances that maintain a thin (0.2-1 μm) gap between the basal PM and a glass. This gap allows free penetration of nutrients and other compounds to basal PM from the bulk culture medium.

The SAE measurements revealed FRET between EphA2-CFP and EphA2-YFP within PM even without stimulation of cells with the EphA2 ligand (Fig 4). Combining this finding with the data of flow cytometry (Fig. 1 b) we can conclude that a fraction of EphA2 forms dimers that are phosphorylated even in the absence of a ligand. These FRET producing EphA2 dimers are distributed over PM rather homogeneously (Fig. 4 b).

Addition of ephrinA3-Fc to cells induced rapid clusterization of EphA2 (Fig 4 b). Such rapid clusterization is in accordance with the data on high mobility of EphA2 in PM (Fig. 3). Formation of clusters was accompanied with fourfold increase in FRET intensity (Fig 4 b,c). FRET intensity reached a maximum in 5-8 min and declined to the initial level in 20-25 min after addition of ephrinA3-Fc (Fig. 4 c). Size and a number of clusters increased during 5-8 min after stimulation of cells with the ligand. At longer time large EphA2 clusters became to disappear from basal PM due to encapsulation of EphA2 in vesicles and their internalization (Fig. 4 b).

From comparison of flow cytometry (Fig. 1 b) and SAE technique data (Fig. 4 c) it is obvious that the kinetics of EphA2 phosphorylation is a little faster than the kinetics of ligand-induced EphA2 dimerization within PM. Here an apparent distortion arises in the order of ligand-induced events because EphA2 phosphorylation must follow receptor dimerization. This inconsistency may be due some peculiarities of experimental setups such as faster binding of ephrinA3-Fc with PM of cells in suspension than with basal PM of adherent cells and delayed breaking of biochemical reactions by paraformaldehyde in phosphorylation studies. Nevertheless, there is a general correlation between flow cytometry (EphA2 phosphorylation) and SAE technique (EphA2 dimerization) results (Fig. 4 c), and our data confirm tentatively the concept that homophilic interactions (i.e. dimerization), clusterization and phosphorylation are closely interrelated steps of ligand-induced functional activation of EphA2.

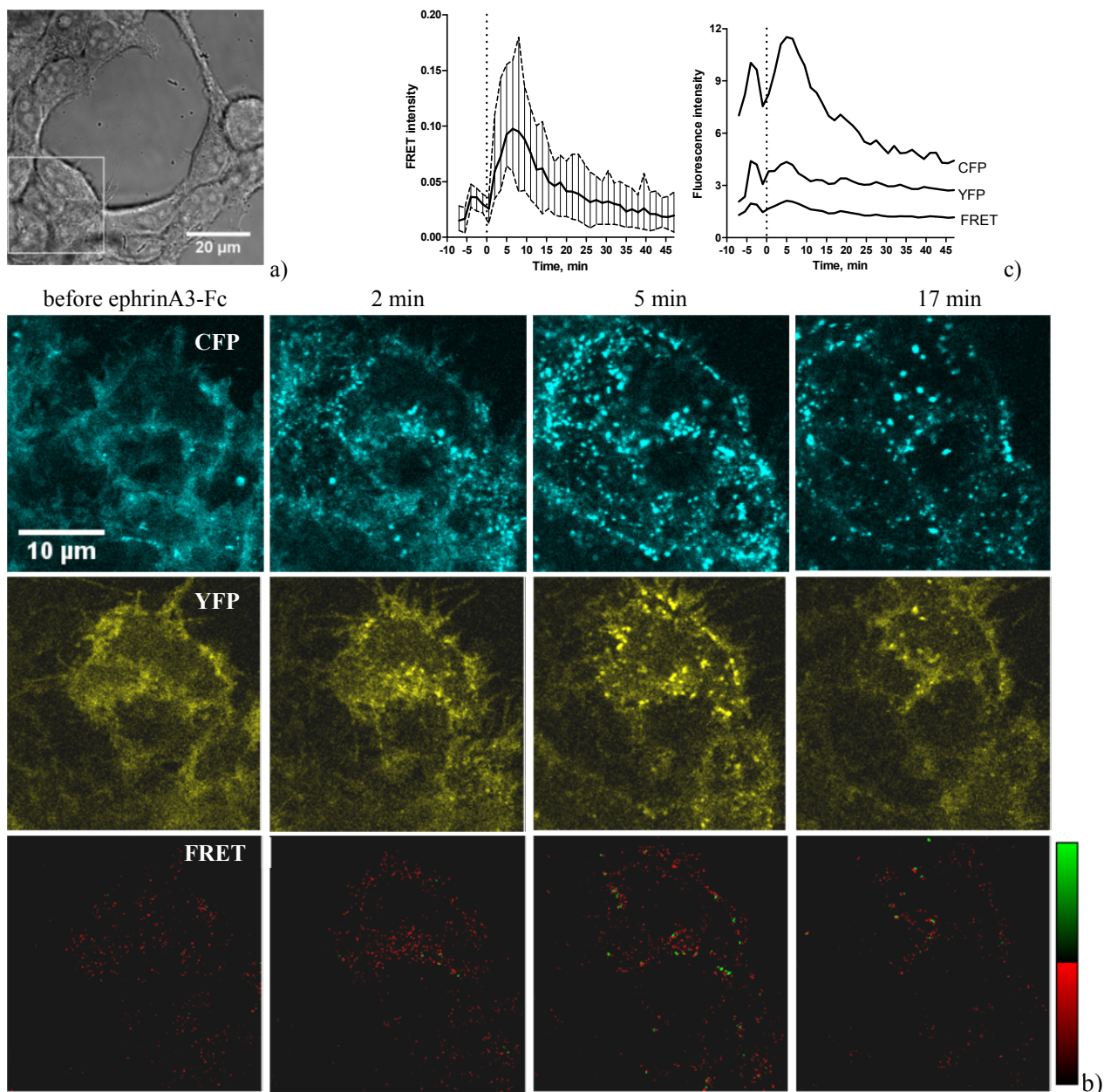


Fig. 4 Clusterization and homodimerization of EphA2 within basal (adjacent to the cover glass) PM of HEK293T cells analyzed by CLSM and SAE technique. a). Transmitted-light image of cells before addition of ephrinA3-Fc. Rectangle indicates an area depicted in b). b). Distribution of EphA2-CFP (upper row), EphA2-YFP (middle row) and FRET signal (bottom row) before and in 2, 5 and 17 min after addition of 10 µg/ml ephrinA3-Fc. Distribution of FRET signal is presented using two-color lookup table. Intensity scale is the same in each row of images. c). Left graph represents mean (bold solid line) and minimum-maximum range of FRET intensity averaged over ten cells as a function of time. Abscissa zero is the time when ephrinA3-Fc was added. On the right graph mean fluorescence intensities of EphA2-CFP, EphA2-YFP and FRET (without correction for crosstalks) are presented.

Acknowledgements The work was supported by Russian foundation for basic research (08-04-01372) and the Program of Cell and Molecular Biology of Russian Academy of Sciences. G.V.S. was supported by the grant of the President of Russian Federation (MK-3160.2008.4). The work was performed in part at User Facilities Center of M.V.Lomonosov Moscow State University.

References

- [1] Lemmon MA, Schlessinger J. Cell signaling by receptor tyrosine kinases. *Cell*. 2010;141(7):1117–1134.
- [2] Bassoni DL, Raab WJ, Achacoso PL, Loh CY, Wehrman TS. Measurements of β -arrestin recruitment to activated seven transmembrane receptors using enzyme complementation. *Methods Mol. Biol.* 2012;897:181–203.
- [3] Blakely BT, Rossi FM, Tillotson B, Palmer M, Estelles A, Blau HM. Epidermal growth factor receptor dimerization monitored in live cells. *Nat. Biotechnol.* 2000;18(2):218–222.
- [4] Lacowicz JR. Principles of fluorescence spectroscopy. New York, NY: Springer; 2006.

- [5] Minor LK. Assays for membrane tyrosine kinase receptors: methods for high-throughput screening and utility for diagnostics. *Expert Review of Molecular Diagnostics*. 2005;5(4):561–571.
- [6] Chudakov DM, Matz MV, Lukyanov S, Lukyanov KA. Fluorescent proteins and their applications in imaging living cells and tissues. *Physiol Rev*. 2010;90(3):1103–1163.
- [7] Lawrence DS, Wang Q. Seeing is believing: peptide-based fluorescent sensors of protein tyrosine kinase activity. *Chembiochem*. 2007;8(4):373–378.
- [8] Wimmer-Kleikamp SH, Janes PW, Squire A, Bastiaens PIH, Lackmann M. Recruitment of Eph receptors into signaling clusters does not require ephrin contact. *J. Cell Biol*. 2004;164(5):661–666.
- [9] Tertoolen LG, Blanchetot C, Jiang G, Overvoorde J, Gadella TW, Hunter T, Hertog J den. Dimerization of receptor protein-tyrosine phosphatase alpha in living cells. *BMC Cell Biology*. 2001;2(1):8.
- [10] Toth PT, Ren D, Miller RJ. Regulation of CXCR4 receptor dimerization by the chemokine SDFf-1 α and the HIV-1 coat protein gp120: a fluorescence resonance energy transfer (FRET) study. *J Pharmacol Exp Ther*. 2004;310(1):8–17.
- [11] Bader AN, Hofman EG, Voortman J, en Henegouwen PMP van B, Gerritsen HC. Homo-FRET imaging enables quantification of protein cluster sizes with subcellular resolution. *Biophys. J*. 2009;97(9):2613–2622.
- [12] Piston DW, Kremers G-J. Fluorescent protein FRET: the good, the bad and the ugly. *Trends Biochem. Sci*. 2007;32(9):407–414.
- [13] Llères D, Swift S, Lamond AI. Detecting protein-protein interactions in vivo with FRET using multiphoton fluorescence lifetime imaging microscopy (FLIM). *Curr Protoc Cytom*. 2007;Chapter 12:Unit12.10.
- [14] Piston DW, Rizzo MA. FRET by fluorescence polarization microscopy. *Methods Cell Biol*. 2008;85:415–430.
- [15] Feige JN, Sage D, Wahli W, Desvergne B, Gelman L. PixFRET, an ImageJ plug-in for FRET calculation that can accommodate variations in spectral bleed-throughs. *Microsc. Res. Tech*. 2005;68(1):51–58.
- [16] Hachet-Haas M, Converset N, Marchal O, Matthes H, Gioria S, Galzi J-L, Lecat S. FRET and colocalization analyzer--a method to validate measurements of sensitized emission FRET acquired by confocal microscopy and available as an ImageJ plug-in. *Microsc. Res. Tech*. 2006;69(12):941–956.
- [17] van Rheenen J, Langeslag M, Jalink K. Correcting confocal acquisition to optimize imaging of fluorescence resonance energy transfer by sensitized emission. *Biophys. J*. 2004;86(4):2517–2529.
- [18] Gordon GW, Berry G, Liang XH, Levine B, Herman B. Quantitative fluorescence resonance energy transfer measurements using fluorescence microscopy. *Biophys. J*. 1998;74(5):2702–2713.
- [19] Chomczynski P, Sacchi N. Single-step method of RNA isolation by acid guanidinium thiocyanate-phenol-chloroform extraction. *Anal. Biochem*. 1987;162(1):156–159.